AGU PUBLICATIONS

JGR

Journal of Geophysical Research: Oceans

RESEARCH ARTICLE

10.1002/2014JC010234

Key Points:

- A new mechanism for deep ocean currents by AGW is presented
- AGW cause chaotic flow trajectories of individual water parcels
- AGW cause stokes drift velocity in the horizontal direction

Correspondence to:
U. Kadri,
ukadri@mit.edu

Citation:
Kadri, U. (2014), Deep ocean water transport by acoustic-gravity waves, *J. Geophys. Res. Oceans*, *119*, 7925–7930, doi:10.1002/2014JC010234.

Received 10 JUN 2014
Accepted 28 OCT 2014
Accepted article online 4 NOV 2014
Published online 24 NOV 2014

Deep ocean water transport by acoustic-gravity waves

Usama Kadri[1]

[1]Department of Mechanical Engineering, Massachusetts Institute of Technology, Cambridge, Massachusetts, USA

Abstract Acoustic-gravity waves are compression-type waves propagating with amplitudes governed by the restoring force of gravity. They are generated, among others, by wind-wave interactions, surface waves interactions, and submarine earthquakes. We show that acoustic-gravity waves contribute to deep ocean currents and circulation; they cause chaotic flow trajectories of individual water parcels, which can be transported up to a few centimeters per second.

1. Introduction

Acoustic-gravity waves (AGW) are compression-type waves propagating with amplitudes governed by the restoring force of gravity. They are generated, among others, by wind-wave interactions, interaction of nearly opposing waves [*Longuet-Higgins*, 1950; *Kedar et al.*, 2008; *Farrell and Munk*, 2010; *Ardhuin et al.*, 2013; *Kadri and Stiassnie*, 2013; *Kadri*, 2015], and submarine earthquakes [*Yamamoto*, 1982]. We show that AGW generate ocean currents and circulations; they cause chaotic flow trajectories of individual water parcels, which can be transported up to a few centimeters per second. With these rates, AGW transport millions of cubic meters of deep water per second.

The vast majority of research on deep ocean currents neglects the slight compressibility of the ocean, which is mostly justified, though not for all applications. Without compressibility, for each frequency ω and constant depth h there can be only a single progressive wave (i.e., *gravity* wave) that corresponds to a wave number κ. However, if the compressibility of the ocean is considered, then for each ω there are m progressive wave modes with horizontal wave numbers κ_n, $n=0, 1, 2, \ldots, m$, where m is the nearest integer smaller than $(\omega h/\pi c+1/2)$, and c is the speed of sound in water [*Kadri and Stiassnie*, 2012]. The first mode, i.e., κ_0, is almost identical to κ of the incompressible case (gravity wave); the other modes, $n=1, 2, \ldots, m$, are called *acoustic-gravity* waves. In fact, any acoustic background might be caused by traveling AGW if h is large enough and the dispersion relation [*Lamb*, 1932]

$$\omega^2=g\lambda_n \tanh(\lambda_n h), \qquad \lambda_n^2=\kappa_n^2-\frac{\omega^2}{c^2}, \tag{1}$$

is satisfied, where λ_n are the eigenvalues of the dispersion relation, and g is the acceleration due to gravity.

2. Deep Orbital Velocities

Consider the two-dimensional problem of a progressive AGW mode, in an ideal compressible ocean. The origin of the Cartesian axes (x, z) is at the undisturbed free surface, where x is in the direction of the propagating surface waves, and z is vertically upward. For an ocean with constant depth and rigid floor, the general linear velocity potential is given by *Longuet-Higgins* [1950, equation (128), p. 22]. For practical purposes, the contribution of the gravitational effects, in the field equation, to the potential, is negligible [see *Longuet-Higgins*, 1950, p. 25]. Ignoring those effects in the field equation (though not in the free surface boundary conditions), yields the simplified two-dimensional compressible velocity potential [e.g., see *Lamb*, 1932],

$$\phi_n=-\frac{H_n}{2}\frac{g}{\omega}\frac{\cosh[\lambda_n(h+z)]}{\cosh(\lambda_n h)}\sin(\kappa_n x-\omega t), \tag{2}$$

or by making use of the dispersion relation (1),

$$\phi_n=-\frac{H_n}{2}\frac{\omega}{\lambda_n}\frac{\cosh[\lambda_n(h+z)]}{\sinh(\lambda_n h)}\sin(\kappa_n x-\omega t), \tag{3}$$

where H_n is the wave height of the nth mode. The horizontal and vertical velocities are then given by

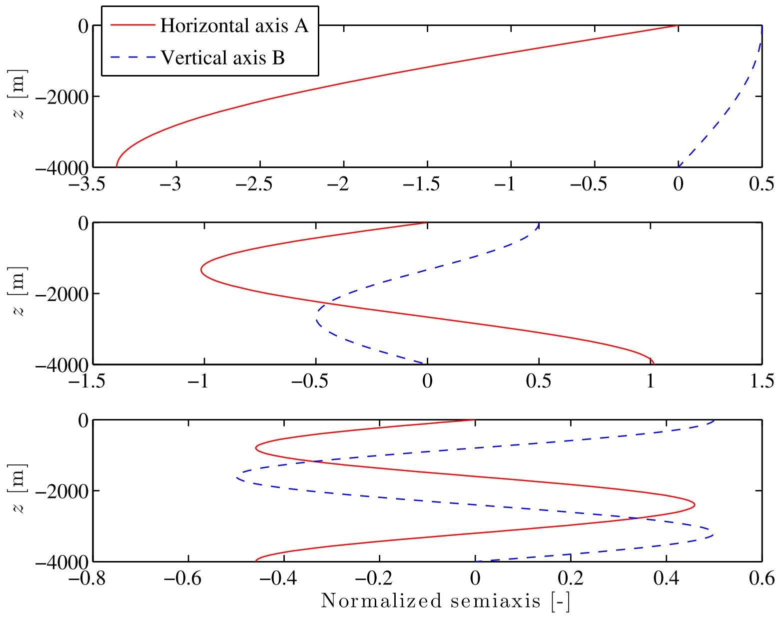

Figure 1. Semiaxes of water particles for AGW (top) mode 1, (middle) mode 2, and (bottom) mode 3; $\omega = 4$ rad/s, $c = 1500$ m/s, $h = 4000$ m, and $g = 9.81$ m/s^2.

$$u_n = -\frac{\partial \phi_n}{\partial x} = \frac{H_n}{2}\frac{\kappa_n}{\lambda_n}\frac{\omega \cosh\left[\lambda_n(h+z)\right]}{\sinh\left(\lambda_n h\right)}\cos\left(\kappa_n x - \omega t\right), \tag{4}$$

$$w_n = -\frac{\partial \phi_n}{\partial z} = \frac{H_n}{2}\frac{\omega \sinh\left[\lambda_n(h+z)\right]}{\sinh\left(\lambda_n h\right)}\sin\left(\kappa_n x - \omega t\right), \tag{5}$$

and the particle displacement components (ξ_n, ζ_n) are found by integrating the velocity with respect to time

$$\xi_n = x_0 - \frac{H_n}{2}\frac{\kappa_n}{\lambda_n}\frac{\cosh\left[\lambda_n(h+z)\right]}{\sinh\left(\lambda_n h\right)}\sin\left(\kappa_n x - \omega t\right), \tag{6}$$

$$\zeta_n = z_0 + \frac{H_n}{2}\frac{\sinh\left[\lambda_n(h+z)\right]}{\sinh\left(\lambda_n h\right)}\cos\left(\kappa_n x - \omega t\right). \tag{7}$$

The displacements (ξ_n, ζ_n) can be rewritten as

$$\begin{aligned}\xi_n(x,z,t) &= -A\sin\left(\kappa_n x - \omega t\right),\\ \zeta_n(x,z,t) &= B\cos\left(\kappa_n x - \omega t\right),\end{aligned} \tag{8}$$

where

$$\left(\frac{\xi_n}{A}\right)^2 + \left(\frac{\zeta_n}{B}\right)^2 = 1, \tag{9}$$

is the equation of an ellipse with a horizontal semiaxis A and a vertical semiaxis B in the x and z directions, respectively. While for surface waves $\lambda_0 \simeq \kappa_0$ is real, and thus the semiaxes decrease exponentially with depth, for AGW λ_n is imaginary and the orbital behavior is periodic with depth, as shown in Figure 1, with $(2m-1)/4$ wavelengths fitting the depth h, where m is the mode number [see also *Jensen et al.*, 2011,

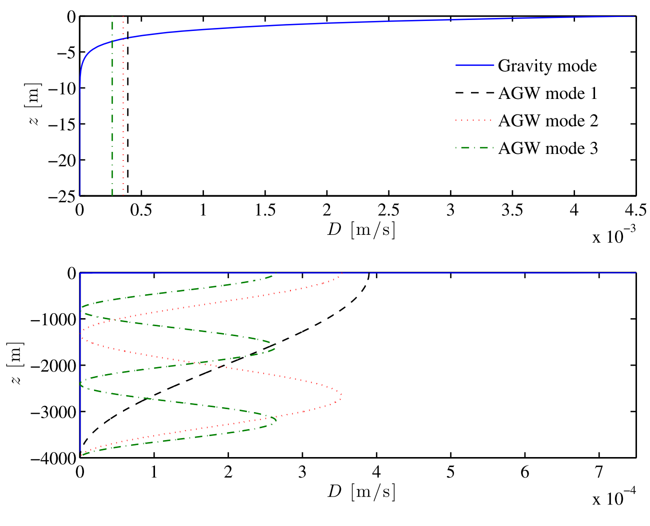

Figure 2. Stokes drift velocities. Gravity waves: $H_1 = 1.5$m, $H_2 = 0.15$m, $\sigma = 2$ rad/s; AGW: $\omega = 4$ rad/s; $c = 1500$ m/s; $h = 4000$ m; $g = 9.81$ m/s^2.

Figure 5.3, p. 267]. Therefore, while surface waves may dominate the flow and net transport of individual water parcels near the surface only, AGW have an additional contribution in the deep ocean as well, where the semiaxes of the low-frequency modes are the longest. Note that λ_n and κ_n are determined by the dispersion relation (1), at a given frequency ω and depth h.

Similarly to surface waves, it is easy to show that AGW experience a *Stokes drift* velocity in the horizontal direction, which is the difference between the mean *Lagrangian* velocity of a fluid parcel, and the mean *Eulerian* velocity of the flow at a fixed location. By using a Taylor expansion of equation (4) about ξ_n to estimate the mean *Lagrangian* velocity, and after simple algebra the Stokes drift velocity in the horizontal direction is finally obtained as

$$D_n(x,z,t)=\frac{\omega\kappa_n H_n^2}{4\sinh^2(\lambda_n h)}\left(\frac{\kappa_n^2}{\lambda_n^2}\cosh^2[\lambda_n(h+z)]\sin^2(\kappa_n x-\omega t)+\sinh^2[\lambda_n(h+z)]\cos^2(\kappa_n x-\omega t)\right). \quad (10)$$

While it is obvious that the gravity wave mode has a contribution near the surface only (see Figure 2, top), AGW cause drift velocities at all depths (see Figure 2, bottom). Averaging over the depth, wavelength $L=2\pi/\kappa$ and period $T=2\pi/\omega$, the mean drift velocity by AGW is calculated by

$$\begin{aligned}\mathbb{D}_n&=\frac{1}{hLT}\int_{-h}^{0}\int_{x}^{x+L}\int_{t}^{t+T}D_n(x,z,t)\,\mathrm{d}z\mathrm{d}x\mathrm{d}t=\\&=\frac{\omega\kappa_n H_n^2}{16\sinh^2(\lambda_n h)}\left[\frac{\kappa_n^2}{\lambda_n^2}\left(\frac{\sinh(2\lambda_n h)}{2\lambda h}+1\right)+\left(\frac{\sinh(2\lambda_n h)}{2\lambda h}-1\right)\right].\end{aligned} \quad (11)$$

The volumetric rate of transport of water parcels by a single AGW is estimated by $Q_n=2\pi Lh\mathbb{D}_n$. Note that in the case of incompressible flow, there is only one progressive wave, i.e., the surface gravity mode. This mode is almost identical to the gravity mode of the compressible case, which decays exponentially with depth. For the incompressible case, substituting $\lambda_0=\kappa_0\equiv\kappa$, $a=H_0/2$, and making use of the dispersion relation, we obtain the well-known Stokes drift velocity [e.g., see *Phillips*, 1977, equation (3.3.5), p. 44], which reduces to $D_0=\omega\kappa a^2 e^{2\kappa z}$ for deep water.

3. Generation by Nonlinear Interaction of Waves

3.1. Resonating Triads

A major source for generating AGW is the interaction of surface gravity waves. Such interaction may lead to resonating triads between two gravity waves and one free AGW that satisfies the dispersion relation (1) [see also *Kadri and Stiassnie*, 2013, equations (3.5)–(3.6)], resulting in energy transfer from the near-surface layer of the ocean. The three waves satisfy the resonance conditions $\kappa_a+\kappa_b=\kappa_c$, and $\omega_a+\omega_b=\omega_c$. The amplitudes of the two gravity waves $A^{(a)}$ and $A^{(b)}$, as well as the amplitude of the AGW $A^{(c)}$ are slowly varying functions of the variable $\zeta=(t-\omega x/\kappa c^2)$. Following *Kadri and Stiassnie* [2013], assuming $|A^{(a)}|>|A^{(b)}|$ an expression for the evolution of $A^{(c)}$ is given by the Jacobian elliptic function

$$|A^{(c)}|=\sqrt{2}|A_0^{(b)}|\mathrm{sn}\left[-(2^{1/2}\sigma^3/g)|A_0^{(a)}|\zeta\ ,\ |A_0^{(b)}|/|A_0^{(a)}|\right], \quad (12)$$

where the subscript zero denotes initial values, and σ is the frequency of the gravity waves ($\omega\simeq 2\sigma$). Note that a detailed derivation of similar evolution equations can be found in *Kadri* [2015]. In the current example, we use the probability density function for the significant wave height H_s developed by *Haver* [1985] based on almost three decades of observations in the North Sea [*Massel*, 1996]:

$$f(H_s)=\begin{cases}\dfrac{1}{\sqrt{2\pi}\sigma_0 H_s}\exp\left[-\dfrac{\left(\ln H_s-\overline{\ln H_s}\right)^2}{2\sigma_0^2 H_s}\right] & \text{for}\quad H_s\le 3.25\text{m}\\[2ex] \beta\dfrac{H_s^{\beta-1}}{\zeta_0^{\beta}}\exp\left[\left(\dfrac{H_s}{\zeta_0}\right)^{\beta}\right], & \text{for}\quad H_s>3.25\text{m}\end{cases} \quad (13)$$

where $\sigma_0^2=0.371$ is the variance and $\overline{\ln H_s}=0.801$ is the mean value of $(\ln H_s)$; and $\beta=1.531$, and $\zeta_0=2.713$, are the Weibull parameters. The probability density function $f(H_s)$ is shown in the first plot of Figure 3, and the corresponding maximum AGW amplitude is calculated by equation (12), i.e., max $|A^{(c)}|=\sqrt{2}|A_0^{(b)}|$

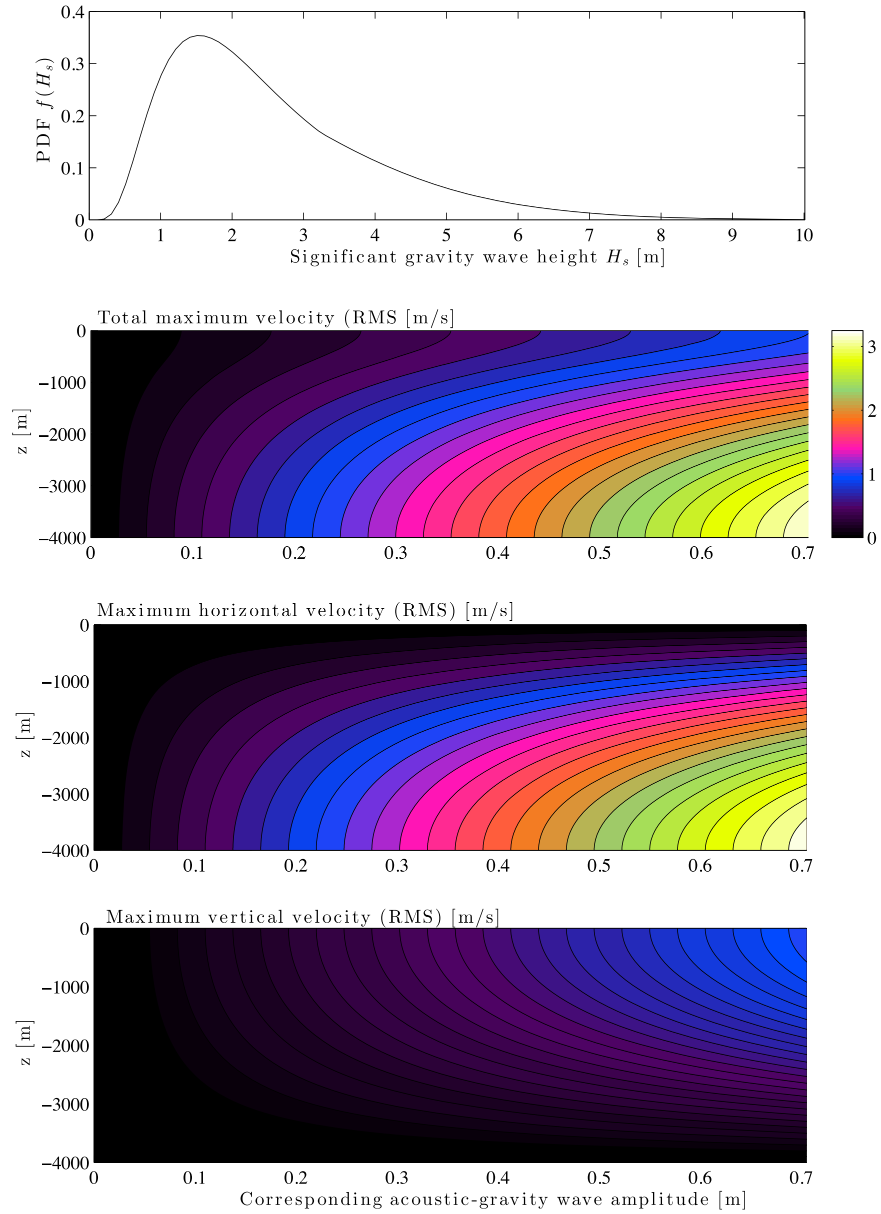

Figure 3. Top-to-bottom: probability density function of the significant gravity wave height; isolines of the maximum total root-mean-square velocity of water particles; isolines of the maximum horizontal root-mean-square velocity of water particles; isolines of the maximum vertical root-mean-square velocity of water particles. $H_1=H_s$; $H_2=0.1H_s$; $\sigma=1$ rad/s; $\omega=2$ rad/s; $c=1500$ m/s; $h=4000$ m; $g=9.81$ m/s^2.

[see *Kadri and Stiassnie*, 2013, equation (7.9)], and $|A_0^{(b)}|=0.1(H_s/2)$, which corresponds to a 10% reflection. Substituting (12) in (4) and (5), the second, third, and fourth plots of Figure 3 show isolines of the maximum root-mean-square total, horizontal, and vertical velocities, induced by the first AGW mode. While the horizontal and vertical velocities increase with the AGW amplitude, the horizontal velocity (of the first mode) increases and the vertical velocity decreases with depth, as can also be concluded from Figure 1, top. Thus, for the first AGW mode, the modal sum of the vector velocity is greatest at the bottom and directed horizontally. Note that the values presented in Figure 3 are for full energy transfer to the first AGW mode. The evolutionary solution with partial energy transfer is presented in the following section.

3.2. Evolution of the Velocity Field

The AGW amplitude $A^{(c)}$ is evolving in time (see equation (12), and Figure 4), and thus the corresponding velocity field is evolutionary. Figure 5 shows isolines of the total root-mean-square velocity of water

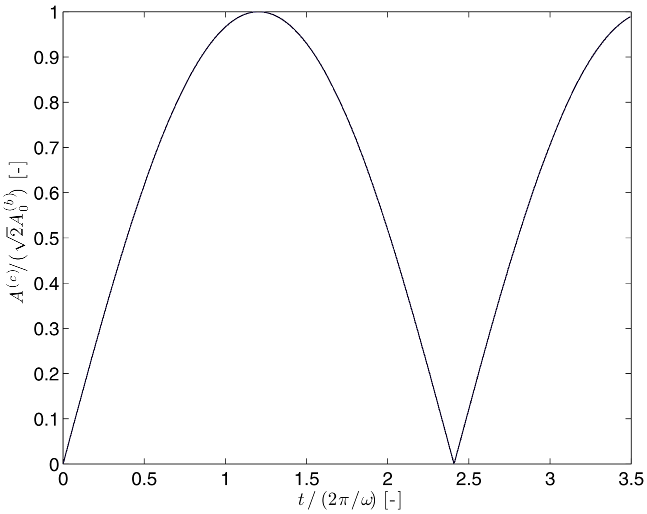

Figure 4. Evolution of an AGW amplitude in resonance with two surface gravity waves in ideal conditions.

particles, in the case of partial energy transfer between the resonating triads that result in say 1%, 5%, or 10% of the maximum amplitude of AGW modes 1, 2, and 3. The range of the maximum induced velocities is of the order of millimeters to decimeters per second, along the ocean depth.

3.3. Stokes Drift Velocity

Consider the problem of AGW generated by two opposing surface gravity waves interacting at normal incident to a shelf break in the x direction. Parallel to the shelf break, in the y direction, there is an effective length l_s along which N AGW are generated, where $N \equiv \lfloor l_s/L \rfloor$. All N AGW of interest propagate away from the shelf break toward the deep sea, causing Stokes drift in the x direction. The total volumetric transport of water parcels by all N AGW is $Q_{tot,n}=N\times Q_n \simeq 2\pi l_s h \mathbb{D}_n$.

In order to quantify the flow drift caused by the AGW take, as an example, $H_a=0.01$m. The corresponding volumetric rates are $Q_1=1.793\times10^4 \mathrm{m}^3/\mathrm{s}$, $Q_2=1.993\times10^3 \mathrm{m}^3/\mathrm{s}$; and $Q_3=7.175\times10^2 \mathrm{m}^3/\mathrm{s}$, for modes 1, 2, and 3, respectively. If the AGW are generated along only 10 km of the shelf break with $N=4$, then the total volumetric rate of the first mode is about $Q_{tot,1}=7.174\times10^4 \mathrm{m}^3/\mathrm{s}$ (0.072 Sv), an amount that is equivalent to 7% of the entire water input from rivers to oceans.

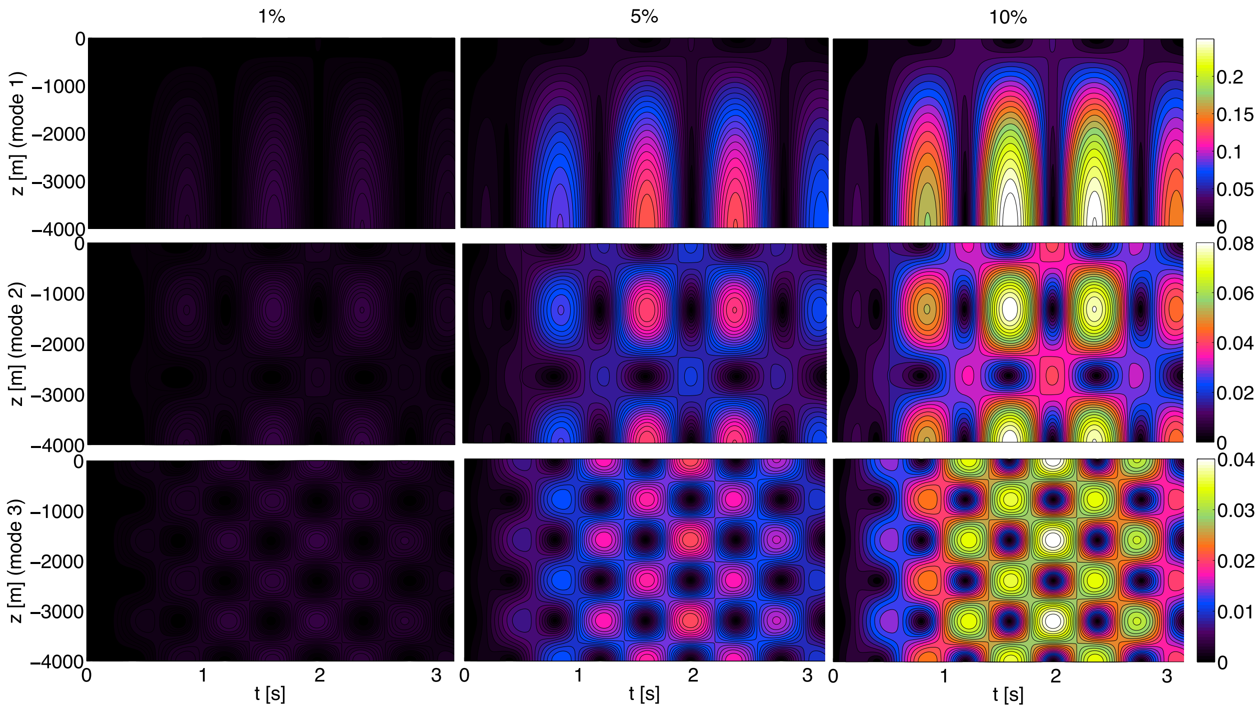

Figure 5. Isolines of the total root-mean-square velocity of water particles. Gravity waves: $H_1=1.5$m, $H_2=0.15$m, $\sigma=2$ rad/s; AGW: $\omega=4$ rad/s; $c=1500$ m/s; $h=4000$ m; $g=9.81$ m/s^2. Columns and rows represent the percentage of energy transferred and the AGW mode, respectively.

3.4. Random Walk

The acoustic spectra levels in the ocean are normally distributed, which indicates random evolution *Duennebier et al.* [2012], i.e., AGW are generated with a random phase shift. As a result, the fluid parcels continuously migrate from one orbit to another while drifting, producing a *random walk*. Depending on the depth and AGW mode the random walk may take place over smaller or larger areas, e.g., the first mode may result in a random walk of just a few decimeters close to the surface, up to tens of meters, in the deep water (see Figure 1, top).

4. Discussion

Acoustic-gravity waves (AGW) can be a major player in transporting water and producing currents at various water depths. The velocity drift and random flow trajectories induced by AGW are probably essential for plankton, algae, bacteria, microorganisms and other marine animals that inhabit the pelagic zone: (1) small drifting microorganisms that cannot swim against a current [*Lalli and Parsons*, 1997] become exposed to larger areas, which enhances their chances of finding food; (2) larger marine animals benefit from the continuous transportation of salt, carbons, nutrients, and other substances that drift with the flow. In particular, this is important for sessile animals, e.g., carnivorous sponges, that live in the deep ocean reaching more than 8000 m [*Vacalet and Boury-Esnault*, 1995].

In principle, the simultaneous generation of many AGW, say along a continental shelf, may result in relatively large currents with volumetric flow rates as great as tens of Sverdrups, which are comparable to the transport of other ocean current systems. Identifying regions of high probability for the generation of AGW from various sources, i.e., wave-wave interactions, tectonic movements, etc., is essential for quantifying the local and global contribution of AGW, a work that requires future multidisciplinary collaborations.

Acknowledgment
I am grateful to Walter Munk for the inspiration, discussions, and feedback on the manuscript; to William Farrell, Meric Srokosz, and an annonymous reviewer for the thorough review and comments; to Carl Wunsch, Raffaeli Ferrari, Andrew Lucas, Michael Stiassnie, Dale Stokes, Sasan Ghaemsaidi for useful discussions, Eric Lauga for hosting me at UCSD, and Triantaphyllos Akylas for hosting me at MIT, where different parts of this research took place, and Anan Kadri for comments on the manuscript. Request for access to the data presented in this paper can be sent to ukadri@mit.edu.

References

Ardhuin, F., T. Lavanant, M. Obrebski, L. Marié, J.-Y. Royer, J.-F. d'Eu, B. M. Howe, R. Lukas, and J. Aucan (2013), A numerical model for ocean ultra-low frequency noise: Wave-generated acoustic-gravity and rayleigh modes, *J. Acoust. Soc. Am.*, *134*(4), 3242–3259.
Duennebier, F. K., R. Lukas, E.-M. Nosal, J. Aucan, and R. A. Weller (2012), Wind, waves, and acoustic background levels at station aloha, *J. Geophys. Res.*, *117*, C03017, doi:10.1029/2011JC007267.
Farrell, W., and W. Munk (2010), Booms and busts in the deep, *J. Phys. Oceanogr.*, *40*(9), 2159–2169.
Haver, S. (1985), Wave climate off northern norway, *Appl. Ocean Res.*, *7*(2), 85–92.
Jensen, F. B., W. A. Kuperman, M. B. Porter, and H. Schmidt (2011), *Computational Ocean Acoustics*, Springer, N. Y.
Kadri, U. (2015), Wave motion in a heavy compressible fluid: Revisited, *Eur. J. Mech.*, *49*, 50–57, doi:10.1016/j.euromechflu.2014.07.008.
Kadri, U., and M. Stiassnie (2012), Acoustic-gravity waves interacting with the shelf break, *J. Geophys. Res.*, *117*, C03035, doi:10.1029/2011JC007674.
Kadri, U., and M. Stiassnie (2013), Generation of an acoustic-gravity wave by two gravity waves, and their subsequent mutual interaction, *J. Fluid Mech.*, *735*, R6, doi:10.1017/jfm.2013.539.
Kedar, S., M. Longuet-Higgins, F. Webb, N. Graham, R. Clayton, and C. Jones (2008), The origin of deep ocean microseisms in the north atlantic ocean, *Proc. R. Soc. A*, *464*(2091), 777–793.
Lalli, C., and T. R. Parsons (1997), *Biological Oceanography: An Introduction*, Butterworth-Heinemann, Oxford, U. K.
Lamb, H. (1932), *Hydrodynamics*, 6th ed., Cambridge Univ. Press, Cambridge, U. K.
Longuet-Higgins, M. S. (1950), A theory of the origin of microseisms, *Philos. Trans. R. Soc. London A*, *243*(857), 1–35.
Massel, S. R. (1996), *Ocean Surface Waves: Their Physics and Prediction*, vol. 11, World Sci., Singapore.
Phillips, O. (1977), *The Dynamics of the Upper Ocean, Cambridge Monogr. on Mech. Appl. Math.*, Cambridge University Press, N. Y.
Vacalet, J., and N. Boury-Esnault (1995), Carnivorous sponges, *Nature*, *373*, 26–43.
Yamamoto, T. (1982), Gravity waves and acoustic waves generated by submarine earthquakes, *Int. J. Soil Dyn. Earthquake Eng.*, *1*(2), 75–82.

